Assessing nodule detection on lung cancer screening in CT: The effects of tube current modulation and model observer selection on detectability maps

J. Hoffman[1], F. Noo[2], K. McMillan[1], S. Young[1], M. McNitt-Gray[1]

[1]Biomedical Physics Interdepartmental Program
University of California Los Angeles, Los Angeles, CA

[2]Department of Radiology
University of Utah, Salt Lake City, UT

SPIE Medical Imaging 2016: Image Perception, Observer Performance, and Technology Assessment

Disclosures

- John Hoffman:
  - Part-time intern, Toshiba Medical Research Institute, USA, Inc.
- Frederic Noo:
  - Insitutional research agreement, Siemens Healthcare
  - Receives research funding from Siemens Healthcare
- Michal McNitt-Gray:
  - Institutional research agreement, Siemens Healthcare
  - Past recipient, research grant support, Siemens Healthcare
  - Consultant, Toshiba America Medical Systems
  - Consultant, Samsung Electronics

Outline

Outline

Outline

Motivation

- Lung cancer is the leading cause of cancer death[1]
- Low-dose CT (LDCT) lung cancer screening has been shown to reduce lung cancer mortality and has recently been approved for use in the US
- Screening scans are performed using low-dose protocols that include the use of tube current modulation (TCM)
- Little is known about the **impact of TCM on detection tasks**

[1] http://www.cdc.gov/cancer/lung/

Motivation

- Lung cancer is the leading cause of cancer death[1]
- Low-dose CT (LDCT) lung cancer screening has been shown to reduce lung cancer mortality and has recently been approved for use in the US
- Screening scans are performed using low-dose protocols that include the use of tube current modulation (TCM)
- Little is known about the **impact of TCM on detection tasks**

[1] http://www.cdc.gov/cancer/lung/

Motivation

- Lung cancer is the leading cause of cancer death[1]
- Low-dose CT (LDCT) lung cancer screening has been shown to reduce lung cancer mortality and has recently been approved for use in the US
- Screening scans are performed using low-dose protocols that include the use of tube current modulation (TCM)
- Little is known about the **impact of TCM on detection tasks**

[1] http://www.cdc.gov/cancer/lung/

Motivation

- Lung cancer is the leading cause of cancer death[1]
- Low-dose CT (LDCT) lung cancer screening has been shown to reduce lung cancer mortality and has recently been approved for use in the US
- Screening scans are performed using low-dose protocols that include the use of tube current modulation (TCM)
- Little is known about the **impact of TCM on detection tasks**

[1] http://www.cdc.gov/cancer/lung/

TCM in screening

- TCM has been shown to lower radiation dose while preserving image quality by
  - **Increasing tube current** in regions/projections of **greater** attenuation
  - **Decreasing tube current** in regions/projections of **lesser** attenuation
- Work has suggested that TCM can impact task-specific detection rates:
  - Gang et al. (2015) [2]: Found a 19% decrease in detectability index detection tasks in head with standard TCM approaches
  - Wunderlich and Noo (2008) [3]: Found that TCM's impact depended on the choice of MO and if channels were used, whether the channels were directional or not
- Lack of thorough studies in anatomically realistic settings and tasks

[2] [Gang et al.,]
[3] [Wunderlich and Noo, 2008]

TCM in screening

- TCM has been shown to lower radiation dose while preserving image quality by
  - **Increasing tube current** in regions/projections of **greater** attenuation
  - **Decreasing tube current** in regions/projections of **lesser** attenuation
- Work has suggested that TCM can impact task-specific detection rates:
  - Gang et al. (2015) [2]: Found a 19% decrease in detectability index detection tasks in head with standard TCM approaches
  - Wunderlich and Noo (2008) [3]: Found that TCM's impact depended on the choice of MO and if channels were used, whether the channels were directional or not
- Lack of thorough studies in anatomically realistic settings and tasks

[2] [Gang et al.,]
[3] [Wunderlich and Noo, 2008]

TCM in screening

- TCM has been shown to lower radiation dose while preserving image quality by
  - **Increasing tube current** in regions/projections of **greater** attenuation
  - **Decreasing tube current** in regions/projections of **lesser** attenuation
- Work has suggested that TCM can impact task-specific detection rates:
  - Gang et al. (2015) [2]: Found a 19% decrease in detectability index detection tasks in head with standard TCM approaches
  - Wunderlich and Noo (2008) [3]: Found that TCM's impact depended on the choice of MO and if channels were used, whether the channels were directional or not
- Lack of thorough studies in anatomically realistic settings and tasks

[2] [Gang et al.,]
[3] [Wunderlich and Noo, 2008]

TCM in screening

- TCM has been shown to lower radiation dose while preserving image quality by
  - **Increasing tube current** in regions/projections of **greater** attenuation
  - **Decreasing tube current** in regions/projections of **lesser** attenuation
- Work has suggested that TCM can impact task-specific detection rates:
  - Gang et al. (2015) [2]: Found a 19% decrease in detectability index detection tasks in head with standard TCM approaches
  - Wunderlich and Noo (2008) [3]: Found that TCM's impact depended on the choice of MO and if channels were used, whether the channels were directional or not
- Lack of thorough studies in anatomically realistic settings and tasks

[2] [Gang et al.,]
[3] [Wunderlich and Noo, 2008]

TCM in screening

- TCM has been shown to lower radiation dose while preserving image quality by
  - **Increasing tube current** in regions/projections of **greater** attenuation
  - **Decreasing tube current** in regions/projections of **lesser** attenuation
- Work has suggested that TCM can impact task-specific detection rates:
  - Gang et al. (2015) [2]: Found a 19% decrease in detectability index detection tasks in head with standard TCM approaches
  - Wunderlich and Noo (2008) [3]: Found that TCM's impact depended on the choice of MO and if channels were used, whether the channels were directional or not
- Lack of thorough studies in anatomically realistic settings and tasks

[2] [Gang et al.,]
[3] [Wunderlich and Noo, 2008]

Outline

Aims

- Assess the **impact of TCM on detection** in simulated lung screening
- Using
  - task-specific formalism
  - realistic data simulation
  - variety of model observers
    - ★ **See if MO selection impacts detection trends**

Outline

Outline

Simulation Methods Overview

- Realistic task (detection of ground glass nodules)
- Computational, anatomical phantom
- Realistic modeling of a clinical scanner
- Extensive noise simulation to achieve good statistics

Simulation Methods Overview

- **Realistic task (detection of ground glass nodules)**
- Computational, anatomical phantom
- Realistic modeling of a clinical scanner
- Extensive noise simulation to achieve good statistics

Task: Ground Glass Nodules

- Hazy, transparent, low-contrast nodules
- Key indicators of cancerous ground glass nodules [Chang et al., 2013]
  - **Growth** of nodule (>2mm increase in size)
  - **Development of part-solid core**
- "Surgical resection leads to excellent prognosis" [Lim et al., 2013]

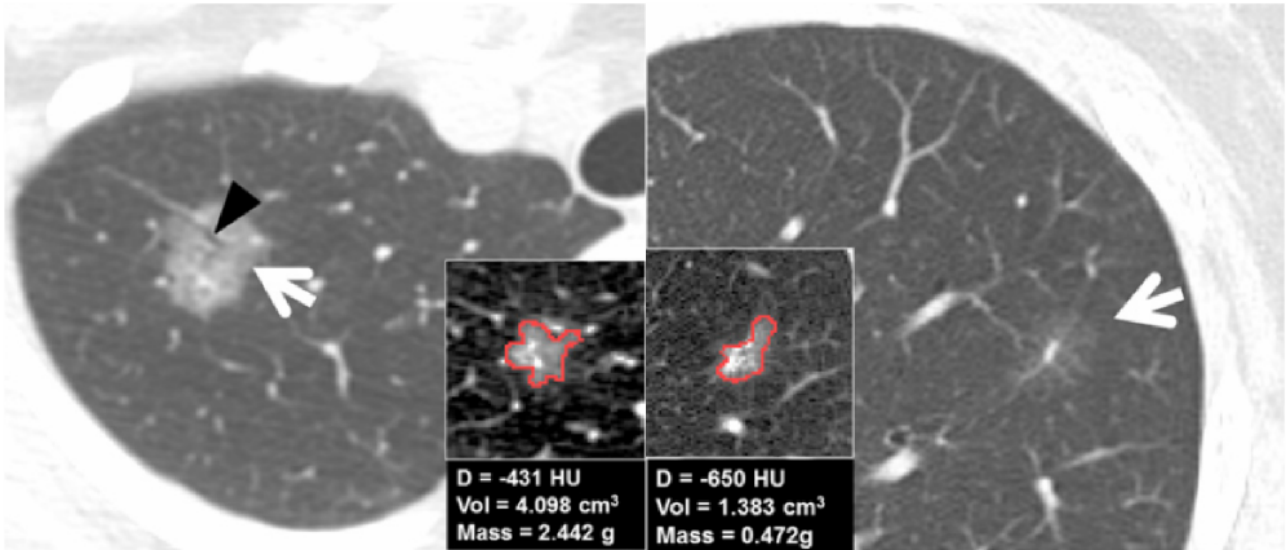

Source: [Lim et al., 2013]

Task: Ground Glass Nodules

- Hazy, transparent, low-contrast nodules
- Key indicators of cancerous ground glass nodules [Chang et al., 2013]
  - **Growth** of nodule (>2mm increase in size)
  - **Development of part-solid core**
- "Surgical resection leads to excellent prognosis" [Lim et al., 2013]

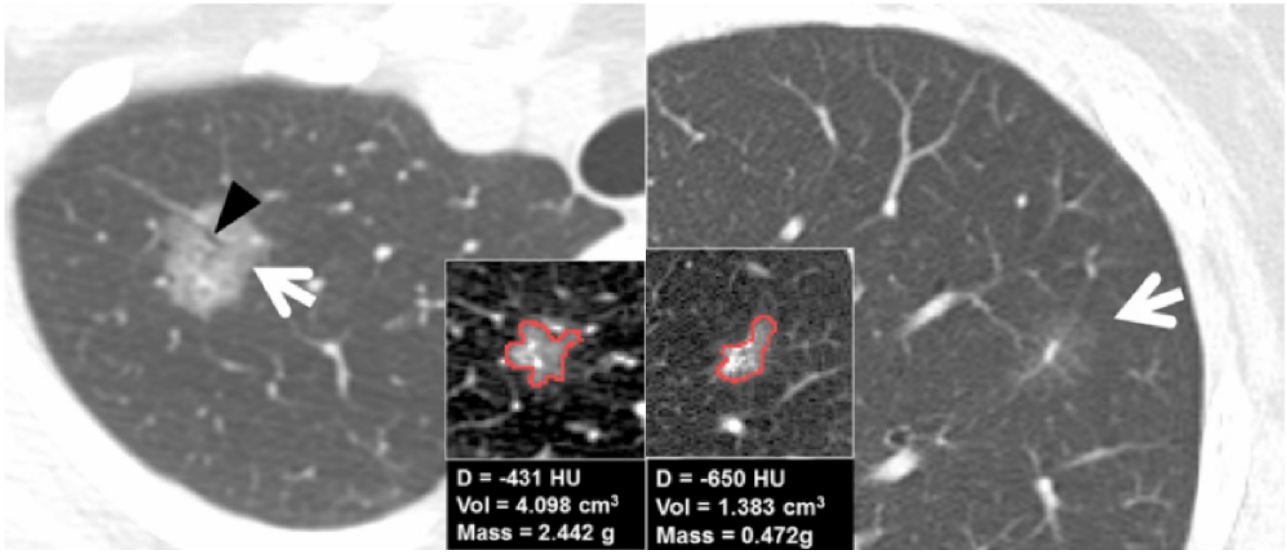

Source: [Lim et al., 2013]

Task: Ground Glass Nodules

- Hazy, transparent, low-contrast nodules
- Key indicators of cancerous ground glass nodules [Chang et al., 2013]
  - **Growth** of nodule (>2mm increase in size)
  - **Development of part-solid core**
- "Surgical resection leads to excellent prognosis" [Lim et al., 2013]

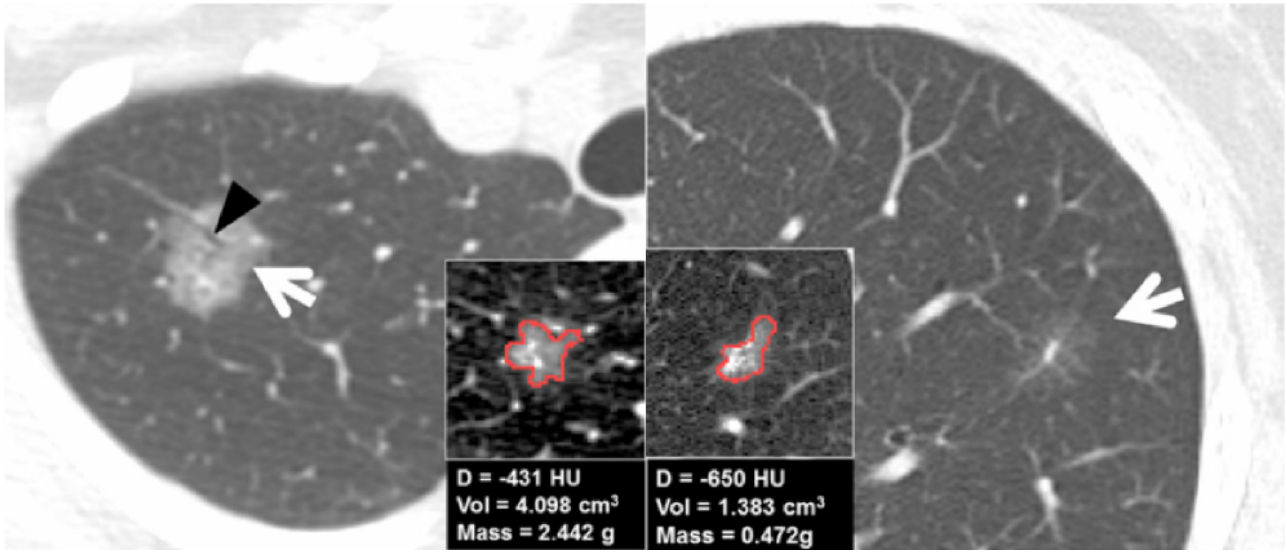

Source: [Lim et al., 2013]

Simulated Nodules

- 6mm diameter, spherical nodules
- 25 HU contrast against background
- One nodule per lung, per scan $\Rightarrow$ 131 "scans"
- 1mm intervals from shoulders to abdomen (z=54mm to z=184mm, respectively)

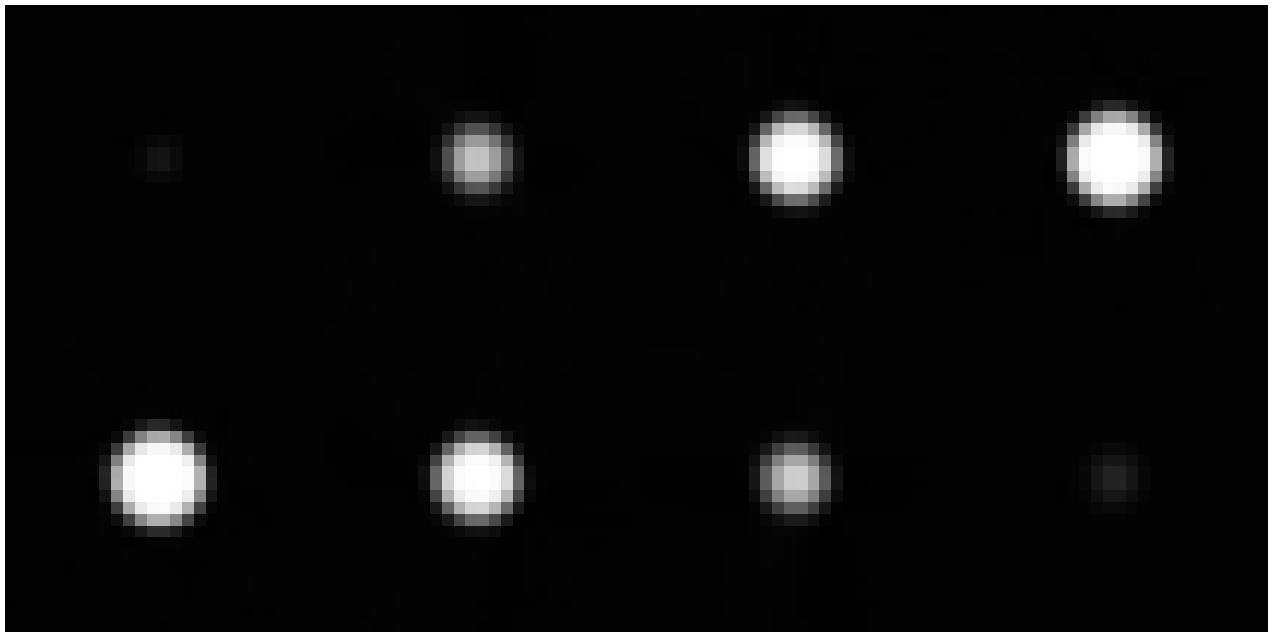

Simulation Methods Overview

- Realistic task (detection of ground glass nodules)
- **Computational, anatomical phantom**
- Realistic modeling of a clinical scanner
- Extensive noise simulation to achieve good statistics

Phantom: The XCAT Phantom[4]

- Anthropomorphic mathematical phantom of thorax
- Voxel values representing physical attenuation values at 80 keV
- No breathing or cardiac motion
- No contrast was simulated

Figure : *Axial, coronal and sagittal views of XCAT phantom*

[4] [Segars et al., 2010]

Simulation Methods Overview

- Realistic task (detection of ground glass nodules)
- Computational, anatomical phantom
- **Realistic modeling of a clinical scanner**
- Extensive noise simulation to achieve good statistics

CT Projection Data

- Sensation 64 geometry
- X-ray source:
  - 80 keV, monochromatic
  - Finite focal spot
  - Tube current modulation*
  - Bowtie filter

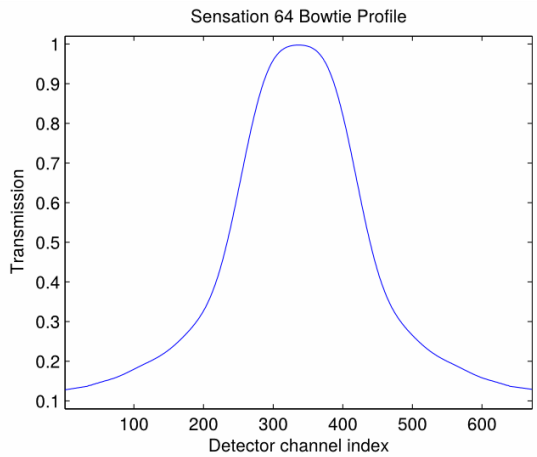

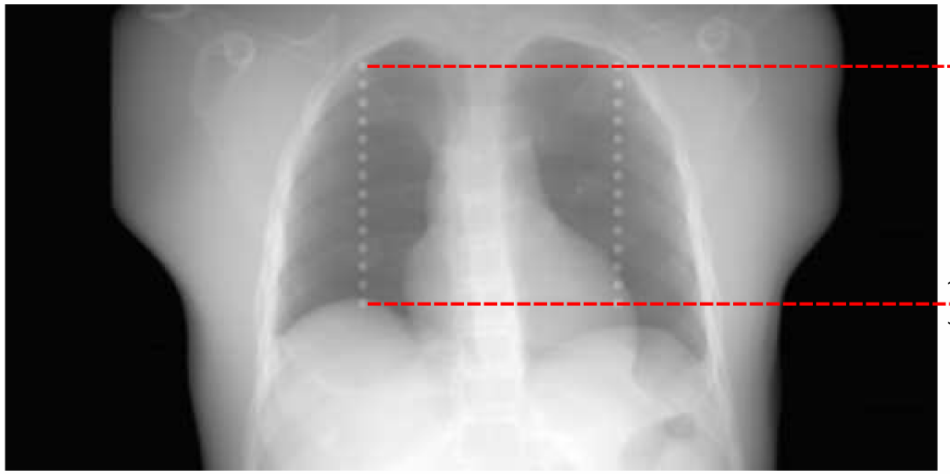

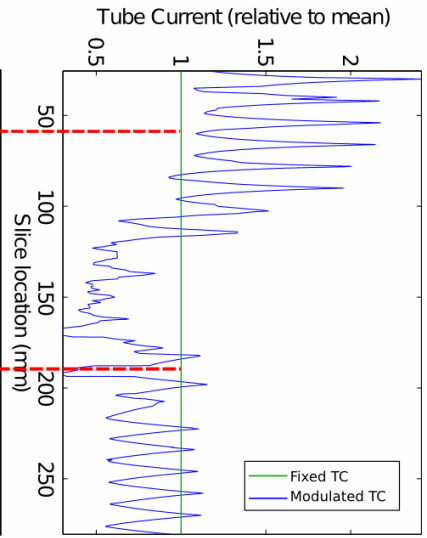

*[Mcmillan et al., 2015]

Simulation Methods Overview

- Realistic task (detection of ground glass nodules)
- Computational, anatomical phantom
- Realistic modeling of a clinical scanner
- **Extensive noise simulation** to achieve good statistics

Simulation Summary

- Using all of the simulation tools described, we simulated
  - 5000 total noise realizations
    - ★ 2500 TCM on
    - ★ 2500 TCM off

Image Reconstruction

- All reconstruction was performed using FreeCT_wFBP [5]
- No iterative reconstruction or denoising
- Reconstructions were performed from **38.5mm** to **199.5 mm** to capture full extent of lung
  - $32 \times 32 \times 54$ voxel volumes ($24 \times 24 \times 162$ mm)
  - Centered on nodules in axial plane
  - 3 mm thick slices
- Nodules simulated and reconstructed separately from noise realizations

[5] http://cvib.ucla.edu/freect; [Hoffman et al., 2016]

Image Reconstruction

- All reconstruction was performed using FreeCT_wFBP [5]
- No iterative reconstruction or denoising
- Reconstructions were performed from **38.5mm** to **199.5 mm** to capture full extent of lung
  - $32 \times 32 \times 54$ voxel volumes ($24 \times 24 \times 162$ mm)
  - Centered on nodules in axial plane
  - 3 mm thick slices
- Nodules simulated and reconstructed separately from noise realizations

[5] http://cvib.ucla.edu/freect; [Hoffman et al., 2016]

Image Reconstruction

- All reconstruction was performed using FreeCT_wFBP [5]
- No iterative reconstruction or denoising
- Reconstructions were performed from **38.5mm** to **199.5 mm** to capture full extent of lung
  - $32 \times 32 \times 54$ voxel volumes ($24 \times 24 \times 162$ mm)
  - Centered on nodules in axial plane
  - 3 mm thick slices
- Nodules simulated and reconstructed separately from noise realizations

[5] http://cvib.ucla.edu/freect; [Hoffman et al., 2016]

Image Reconstruction

- All reconstruction was performed using FreeCT_wFBP [5]
- No iterative reconstruction or denoising
- Reconstructions were performed from **38.5mm** to **199.5 mm** to capture full extent of lung
  - $32 \times 32 \times 54$ voxel volumes ($24 \times 24 \times 162$ mm)
  - Centered on nodules in axial plane
  - 3 mm thick slices
- Nodules simulated and reconstructed separately from noise realizations

[5] http://cvib.ucla.edu/freect; [Hoffman et al., 2016]

Outline

Detection Task

- Signal known exactly/background known exactly (SKE/BKE)
- Assume: all noise is gaussian
  - $\Rightarrow$Test statistic is Gaussian
  - $\Rightarrow$Variance in class 1 (signal absent) and class 2 (signal present) statistics can be assumed to be equal without introducing significant error [6]
- Thus, can go directly from ensemble images$\rightarrow$SNR$\rightarrow$AUC

I.e.:

$$SNR^2 = \Delta \mathbf{s}^t \mathbf{K}_n^{-1} \Delta \mathbf{s}$$

$$AUC = \frac{1}{2} + \frac{1}{2}\mathrm{erf}\left(\frac{SNR}{2}\right) = \frac{1}{2} + \frac{1}{2}\mathrm{erf}\left(\frac{\sqrt{\Delta \mathbf{s}^t \mathbf{K}_n^{-1} \Delta \mathbf{s}}}{2}\right)$$

[6] [Wunderlich and Noo, 2011]

Detection Task

- Signal known exactly/background known exactly (SKE/BKE)
- Assume: all noise is gaussian
  - $\Rightarrow$Test statistic is Gaussian
  - $\Rightarrow$Variance in class 1 (signal absent) and class 2 (signal present) statistics can be assumed to be equal without introducing significant error [6]
- Thus, can go directly from ensemble images$\rightarrow$SNR$\rightarrow$AUC

I.e.:

$$SNR^2 = \Delta \mathbf{s}^t \mathbf{K}_n^{-1} \Delta \mathbf{s}$$

$$AUC = \frac{1}{2} + \frac{1}{2}\mathrm{erf}\left(\frac{SNR}{2}\right) = \frac{1}{2} + \frac{1}{2}\mathrm{erf}\left(\frac{\sqrt{\Delta \mathbf{s}^t \mathbf{K}_n^{-1} \Delta \mathbf{s}}}{2}\right)$$

[6] [Wunderlich and Noo, 2011]

Detection Task

- Signal known exactly/background known exactly (SKE/BKE)
- Assume: all noise is gaussian
  - $\Rightarrow$Test statistic is Gaussian
  - $\Rightarrow$Variance in class 1 (signal absent) and class 2 (signal present) statistics can be assumed to be equal without introducing significant error [6]
- Thus, can go directly from ensemble images$\rightarrow$SNR$\rightarrow$AUC

I.e.:

$$SNR^2 = \Delta \mathbf{s}^t \mathbf{K}_n^{-1} \Delta \mathbf{s}$$

$$AUC = \frac{1}{2} + \frac{1}{2}\text{erf}\left(\frac{SNR}{2}\right) = \frac{1}{2} + \frac{1}{2}\text{erf}\left(\frac{\sqrt{\Delta \mathbf{s}^t \mathbf{K}_n^{-1} \Delta \mathbf{s}}}{2}\right)$$

[6] [Wunderlich and Noo, 2011]

Detectability Maps

- Reminder: our aim is to

  Investigate TCM's impact on regional nodule detection

- Use AUC from different MOs as a metric for detectability

  Does MO selection impact trends in detectability?

- **Detectability maps**
  - Plots of AUC as a function of nodule location

Detectability Maps

- Reminder: our aim is to

  Investigate TCM's impact on regional nodule detection

- Use AUC from different MOs as a metric for detectability

  Does MO selection impact trends in detectability?

- Detectability maps
  - Plots of AUC as a function of nodule location

Detectability Maps

- Reminder: our aim is to

  Investigate TCM's impact on regional nodule detection

- Use AUC from different MOs as a metric for detectability

  Does MO selection impact trends in detectability?

- Detectability maps
  - Plots of AUC as a function of nodule location

Detectability Maps

- Reminder: our aim is to

  Investigate TCM's impact on regional nodule detection

- Use AUC from different MOs as a metric for detectability

  Does MO selection impact trends in detectability?

- **Detectability maps**
  - Plots of AUC as a function of nodule location

Sample Detectability Map

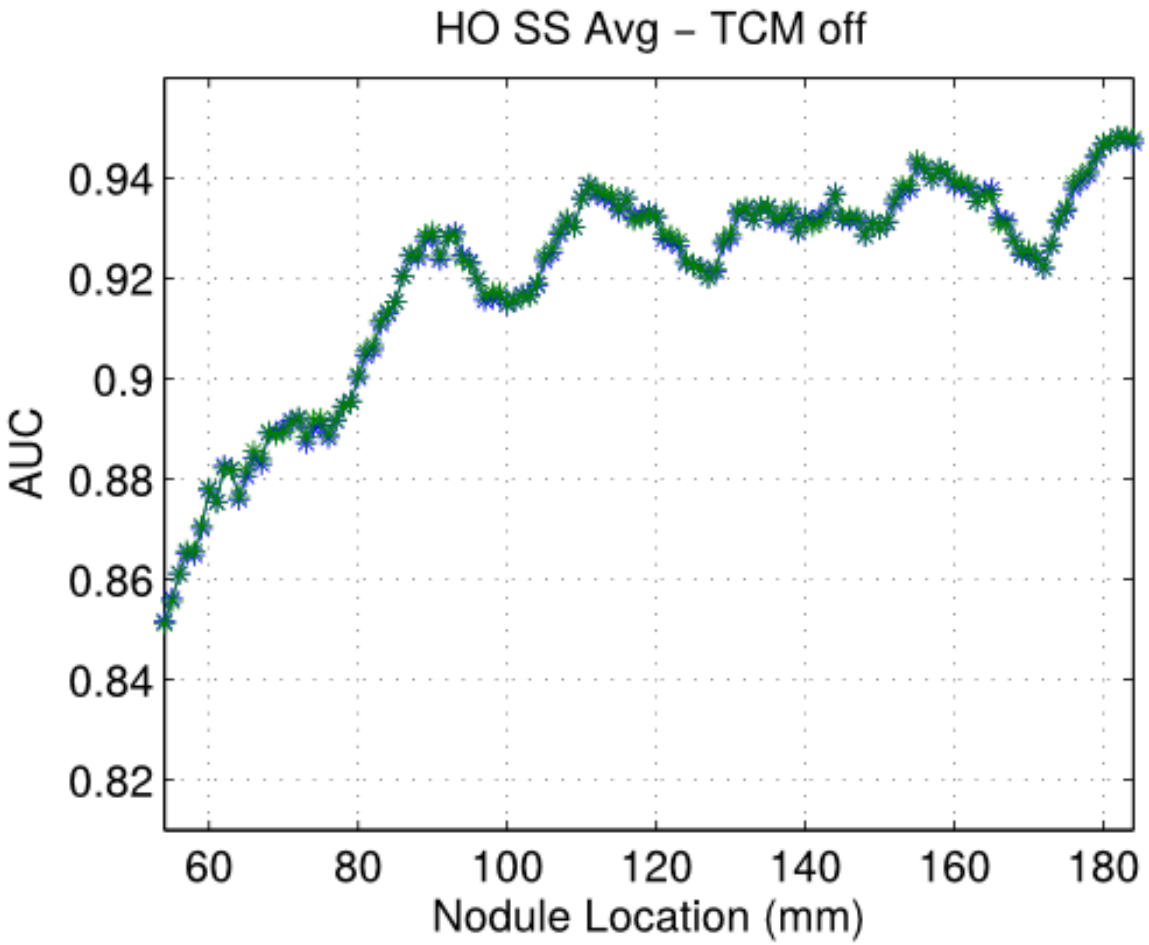

Sample Detectability Map

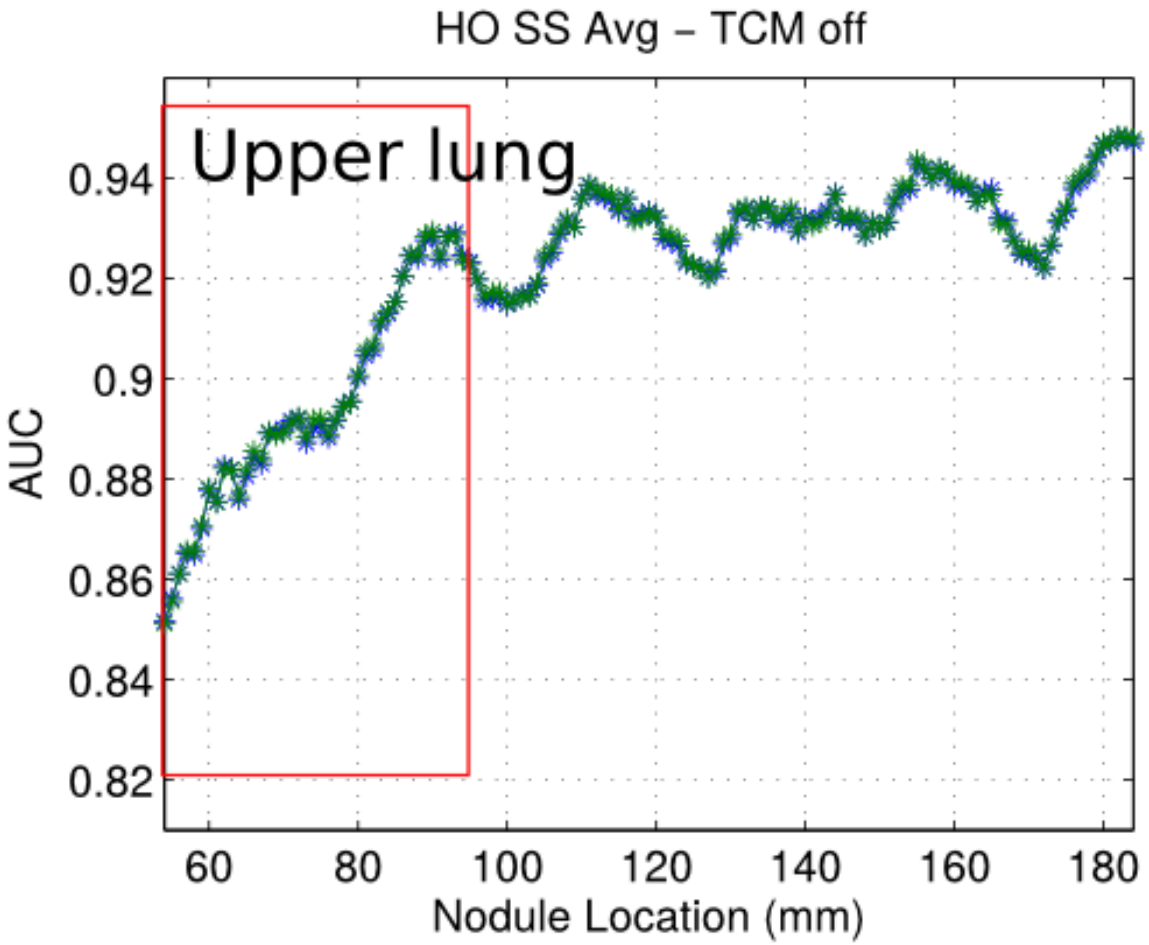

Sample Detectability Map

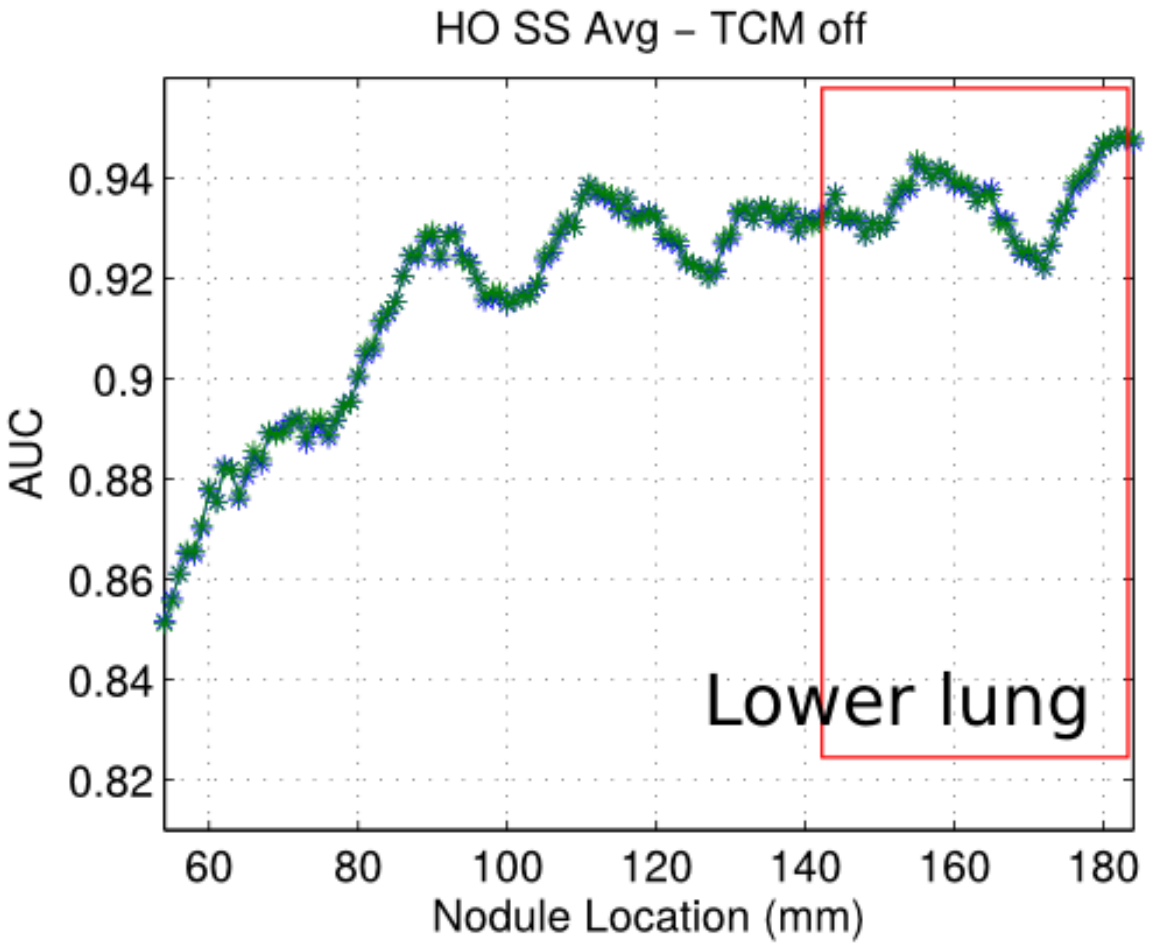

Sample Detectability Map

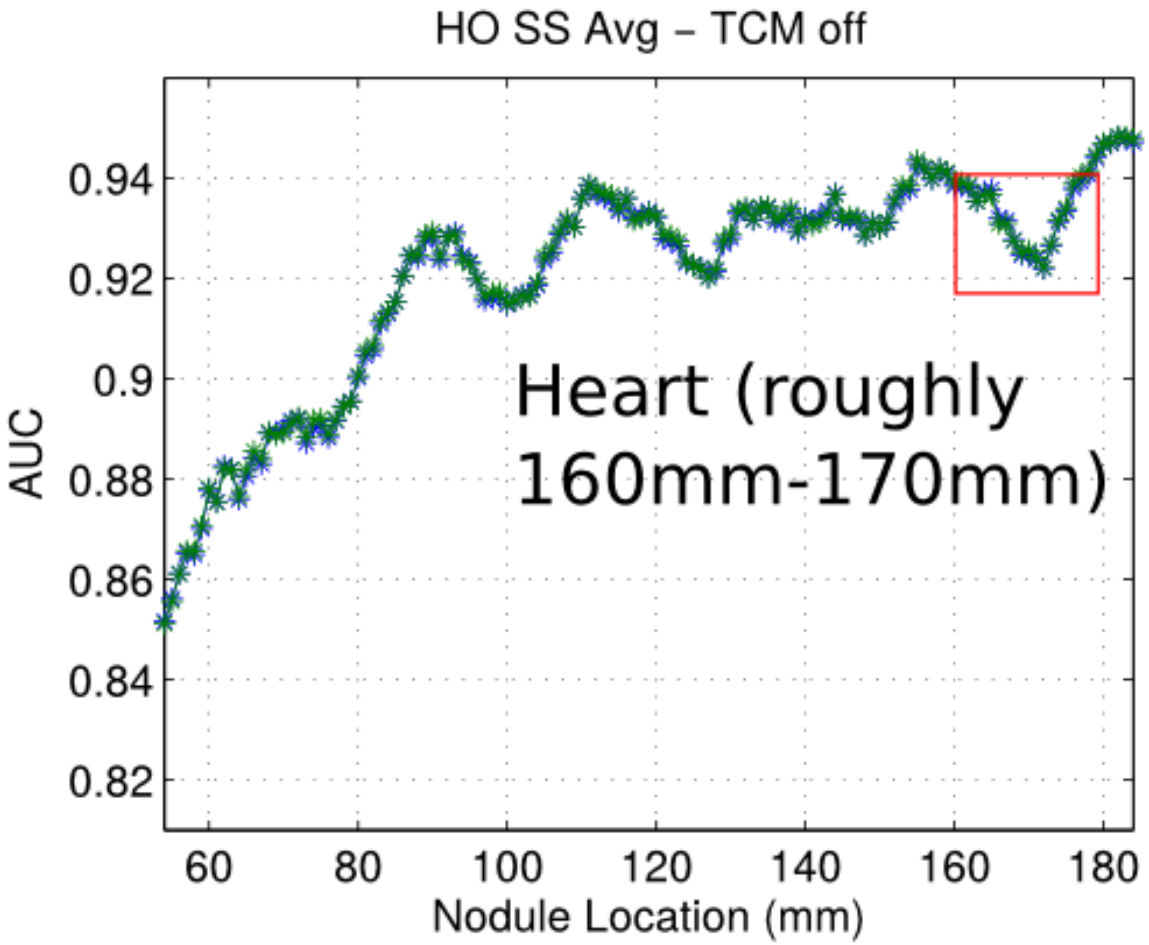

Model observers

- To produce our AUC statistics, we utilized a variety of model observers...

Model Observers

- "Single" Slice (MOs run on 2D image data)
  - Average
    - ★ Hotelling observer
    - ★ Channelized Hotelling observer
  - Central Slice
    - ★ Hotelling observer
    - ★ Channelized Hotelling observer
- Volumetric (Fully 3D MOs)
  - Hotelling observer
  - Non-prewhitening matched filter
- Multislice (Hybrid 2D/3D)
  - Channelized hotelling in XY & NPWMF in Z

Model Observers

- "Single" Slice (MOs run on 2D image data)
  - Average
    - ★ **Hotelling observer**
    - ★ **Channelized Hotelling observer**
  - Central Slice
    - ★ Hotelling observer
    - ★ Channelized Hotelling observer
- Volumetric (Fully 3D MOs)
  - Hotelling observer
  - Non-prewhitening matched filter
- Multislice (Hybrid 2D/3D)
  - **Channelized hotelling in XY & NPWMF in Z**

Model Observers

- **"Single" Slice** (MOs run on 2D image data)
  - **Average**
    - ★ Hotelling observer
    - ★ Channelized Hotelling observer
  - Central Slice
    - ★ Hotelling observer
    - ★ Channelized Hotelling observer
- Volumetric (Fully 3D MOs)
  - Hotelling observer
  - Non-prewhitening matched filter
- Multislice (Hybrid 2D/3D)
  - Channelized hotelling in XY & NPWMF in Z

Single-slice Averaging

- Compress volumetric data into a single slice by taking average of all slices, then run MO
  - Hotelling observer
  - Channelized Hotelling observer

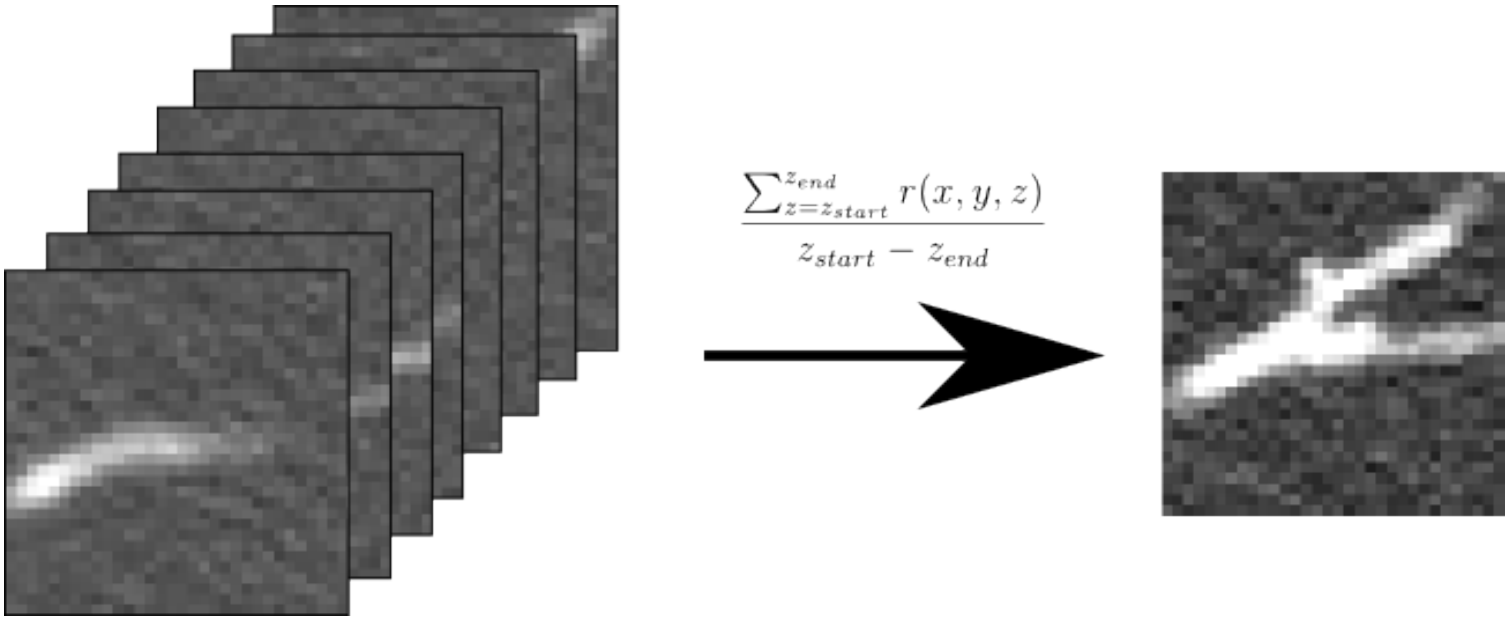

Model Observers

- "Single" Slice (MOs run on 2D image data)
  - Average
    - ★ **Hotelling observer**
    - ★ Channelized Hotelling observer
  - Central Slice
    - ★ Hotelling observer
    - ★ Channelized Hotelling observer
- Volumetric (Fully 3D MOs)
  - Hotelling observer
  - Non-prewhitening matched filter
- Multislice (Hybrid 2D/3D)
  - Channelized hotelling in XY & NPWMF in Z

Hotelling Observer

Hotelling Observer (with Gaussian noise)

$$\lambda_{HO}(\mathbf{g}) = \Delta\mathbf{s}^t \mathbf{K}_n^{-1} \mathbf{g}$$

$$SNR_\lambda^2 = \Delta\mathbf{s}^t \mathbf{K}_n^{-1} \Delta\mathbf{s}$$

$$SNR^2 = \text{  }^T \text{cov}(\text{ 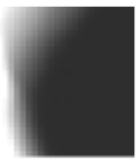 })^{-1} \text{  }$$

Model Obervers

- "Single" Slice (MOs run on 2D image data)
  - Average
    - ★ Hotelling observer
    - ★ **Channelized Hotelling observer**
  - Central Slice
    - ★ Hotelling observer
    - ★ Channelized Hotelling observer
- Volumetric (Fully 3D MOs)
  - Hotelling observer
  - Non-prewhitening matched filter
- Multislice (Hybrid 2D/3D)
  - Channelized hotelling in XY & NPWMF in Z

Channelized Observers

- Channelize using 40 Gabor Channels [7]

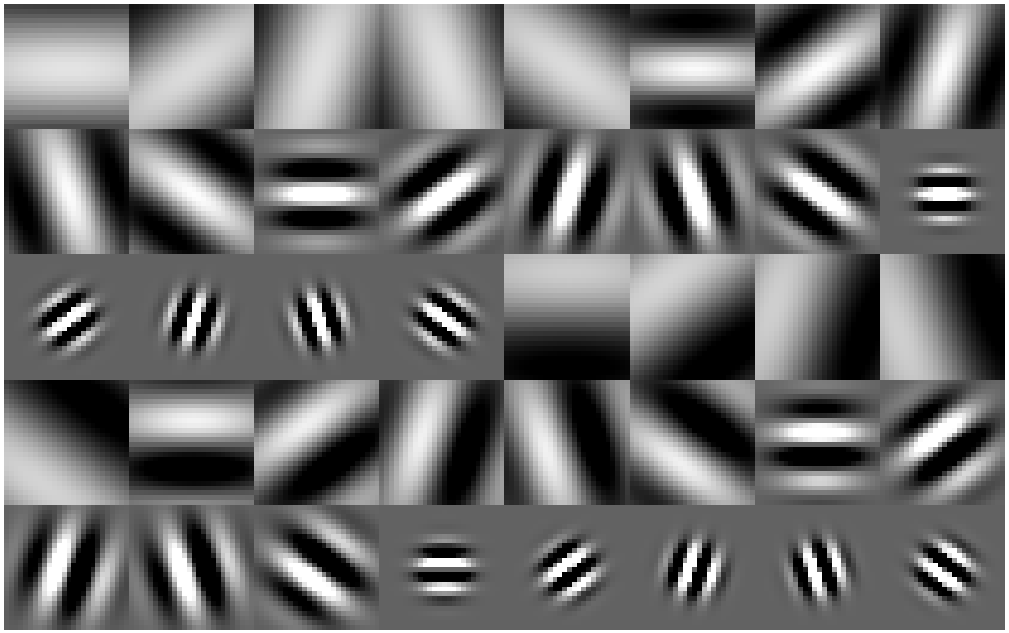

- Internal observer noise added as a multiplicative factor to the diagonal of the covariance matrix:

$$\mathbf{K}_{\text{internal noise}} = \mathbf{K} + 0.75 \times \text{diag}(\mathbf{K})$$

[7] Channels created using IQmodelo: https://github.com/DIDSR/IQmodelo

Channelized Observers

- Channelize using 40 Gabor Channels [7]

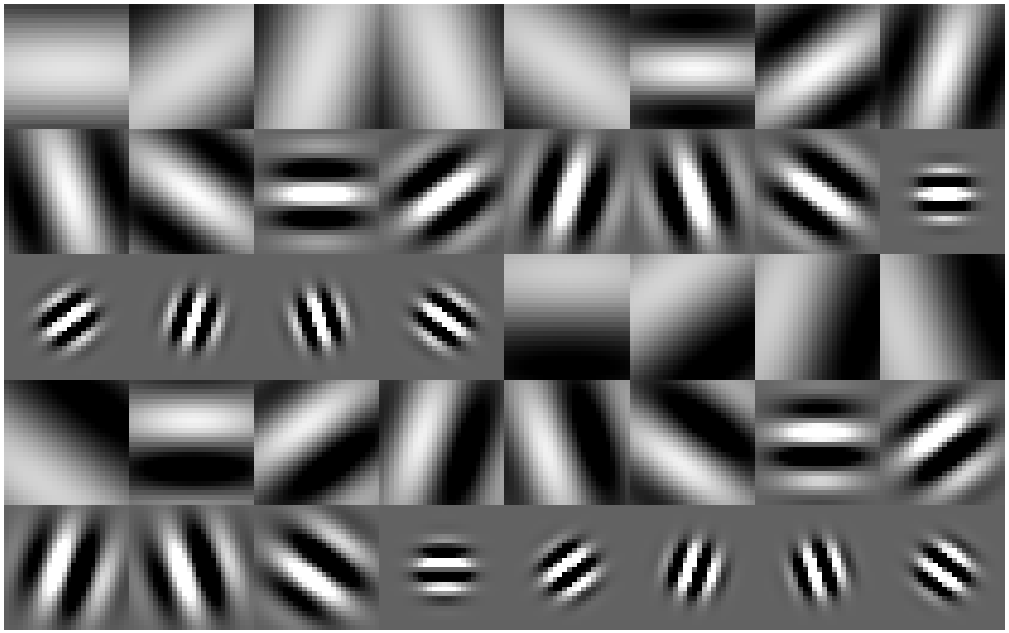

- Internal observer noise added as a multiplicative factor to the diagonal of the covariance matrix:

$$\mathbf{K}_{\text{internal noise}} = \mathbf{K} + 0.75 \times \text{diag}(\mathbf{K})$$

[7] Channels created using IQmodelo: https://github.com/DIDSR/IQmodelo

Channelized Hotelling Observer (CHO)

Channelized Hotelling observer

$$\lambda_{CHO} = \omega_{CHO}^t \mathbf{g}_c$$

$$SNR_{CHO}^2 = \Delta\bar{\mathbf{s}}_c^t \mathbf{K}_{c,n}^{-1} \Delta\bar{\mathbf{s}}_c$$

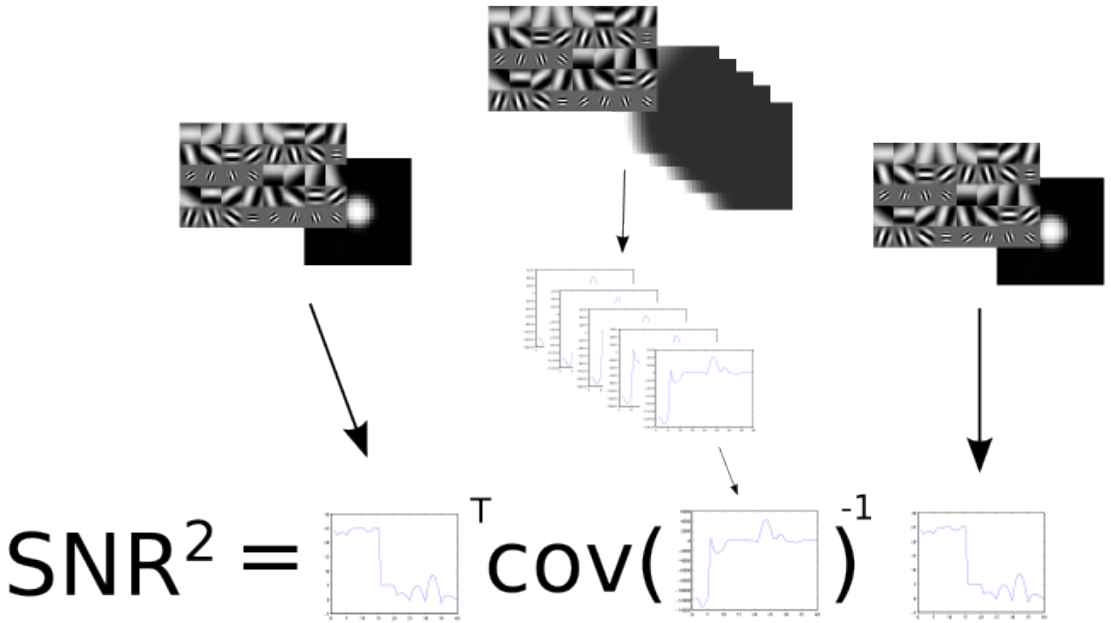

Model Obervers

- "Single" Slice (MOs run on 2D image data)
  - Average
    - ★ Hotelling observer
    - ★ Channelized Hotelling observer
  - Central Slice
    - ★ Hotelling observer
    - ★ Channelized Hotelling observer
- Volumetric (Fully 3D MOs)
  - Hotelling observer
  - Non-prewhitening matched filter
- Multislice (Hybrid 2D/3D)
  - **Channelized hotelling in XY & NPWMF in Z**

Multi-slice CHO

- Multi-slice Channelized Hotelling Observer "C" [8]
  - All slices are channelized individually
  - Channelized slices are fed into 1D Hotelling observer

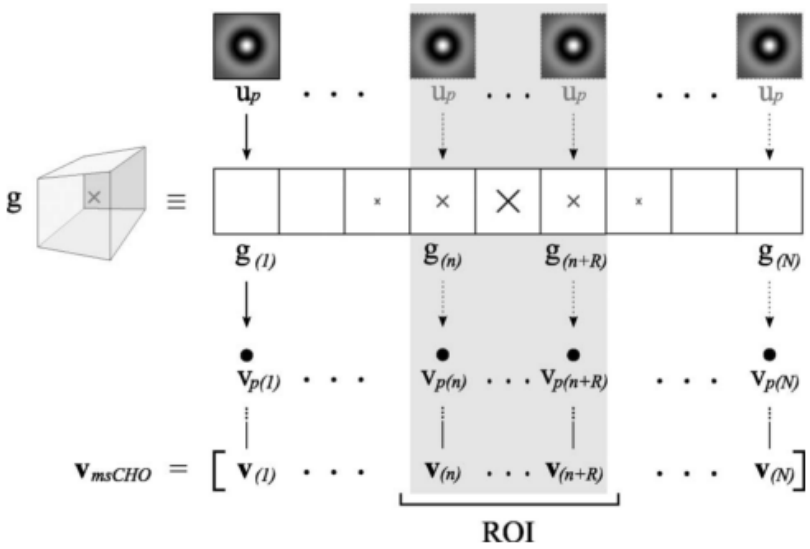

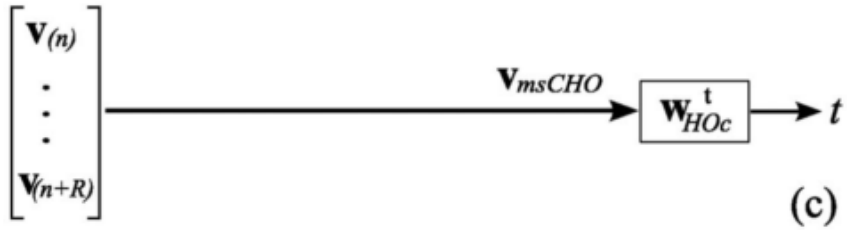

Image source: [Platiša et al., 2011]

[8] [Platiša et al., 2011]

Multislice Observer

- Better than single slice observers, but not fully three-dimensional
- Benefits:
  - Perhaps closer to how human observers integrate volumetric data
  - Channelization helps limit the size of the covariance matrix compared to a volumetric HO
  - Better statistics when data is limited

Multislice Observer

- Better than single slice observers, but not fully three-dimensional
- Benefits:
  - Perhaps closer to how human observers integrate volumetric data
  - Channelization helps limit the size of the covariance matrix compared to a volumetric HO
  - Better statistics when data is limited

We want to use these MOs to answer the following

1. Does TCM use impact the regional detectability of nodules in the lung?
2. Does MO selection affect any observed trends?

We want to use these MOs to answer the following

1. Does TCM use impact the regional detectability of nodules in the lung?
2. Does MO selection affect any observed trends?

Outline

Outline

Single-slice-average Hotelling Observer

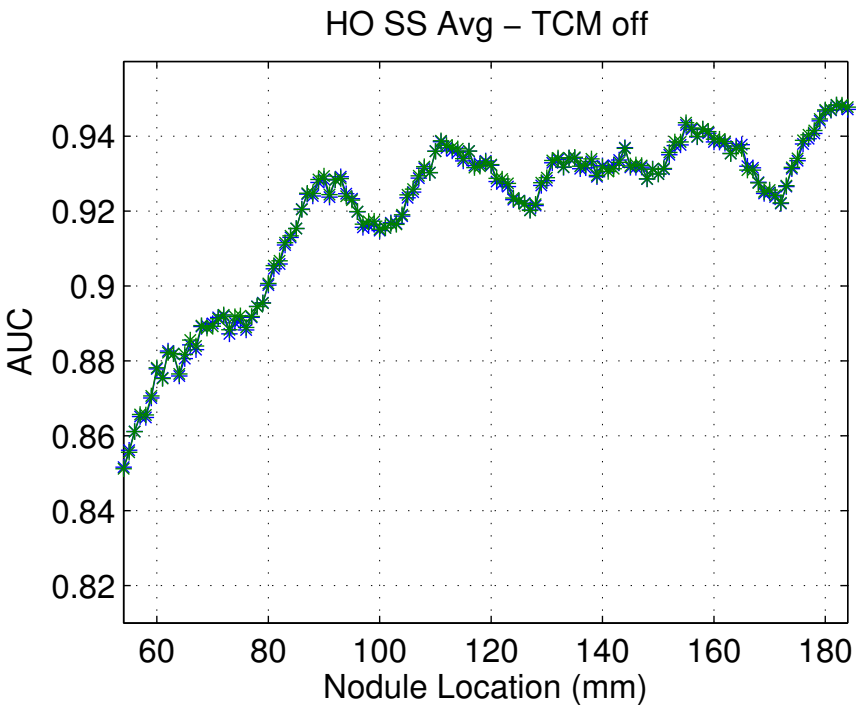

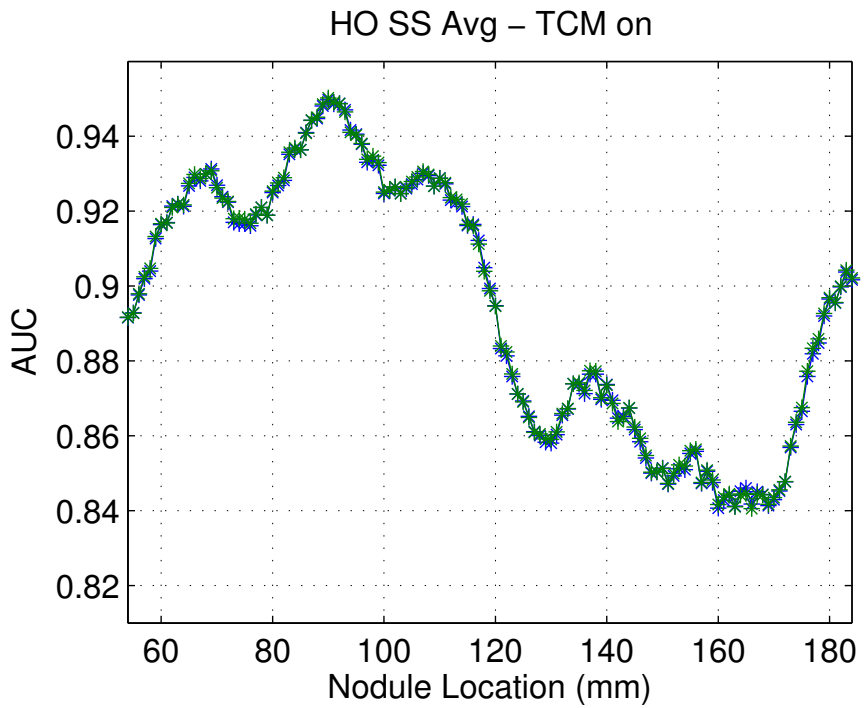

- Fixed Tube current: detection lowest in shoulders, highest in lower lung
- TCM: detection highest in shoulders, lowest in mid-lower lung, increasing into the abdomen

CHO Single Slice Average

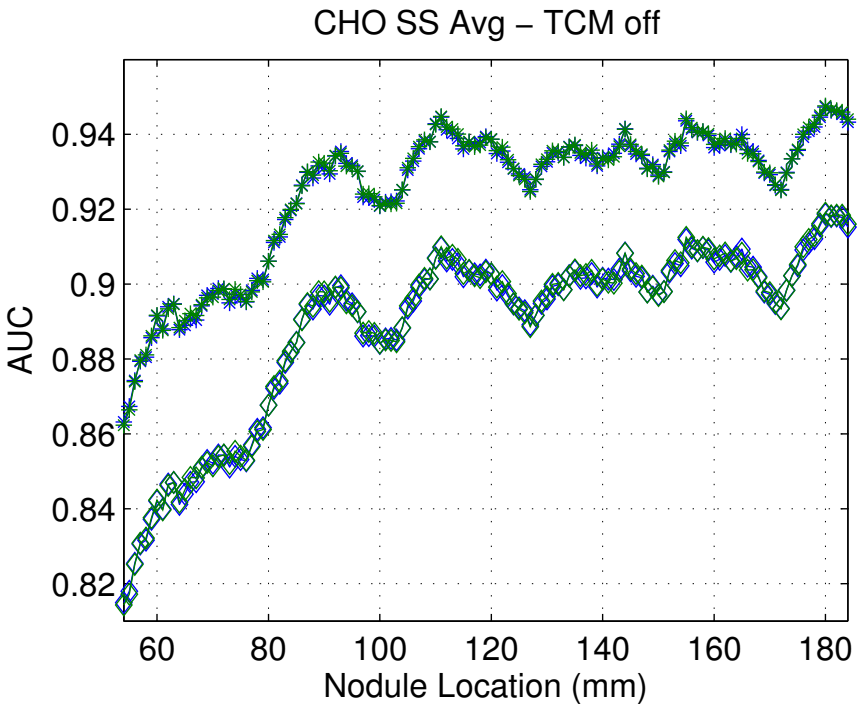

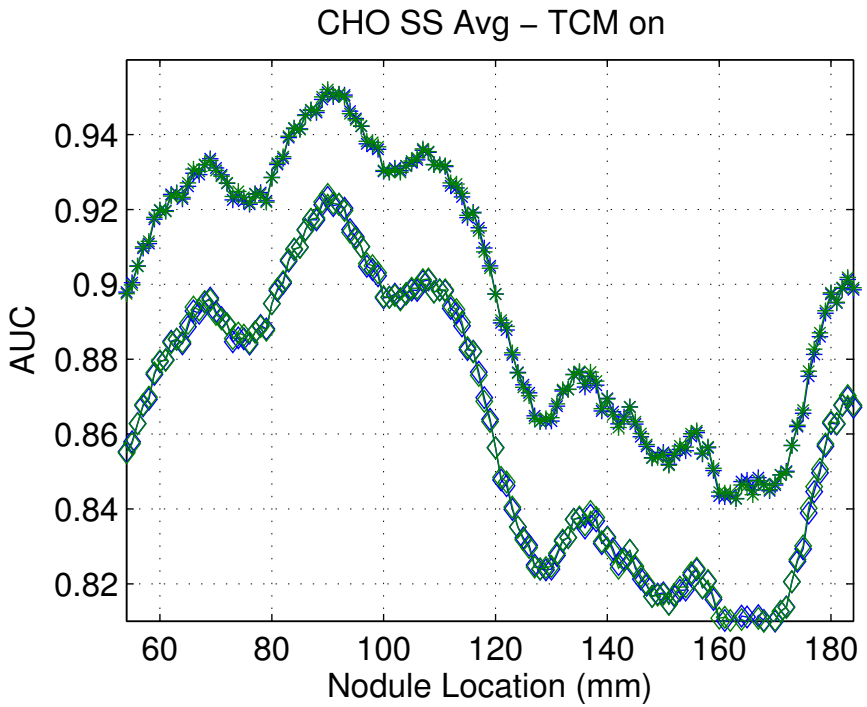

- Trends same as single-slice averaged HO
- Internal noise lowers detection, however does not impact trends

Outline

Multi-slice CHO Results

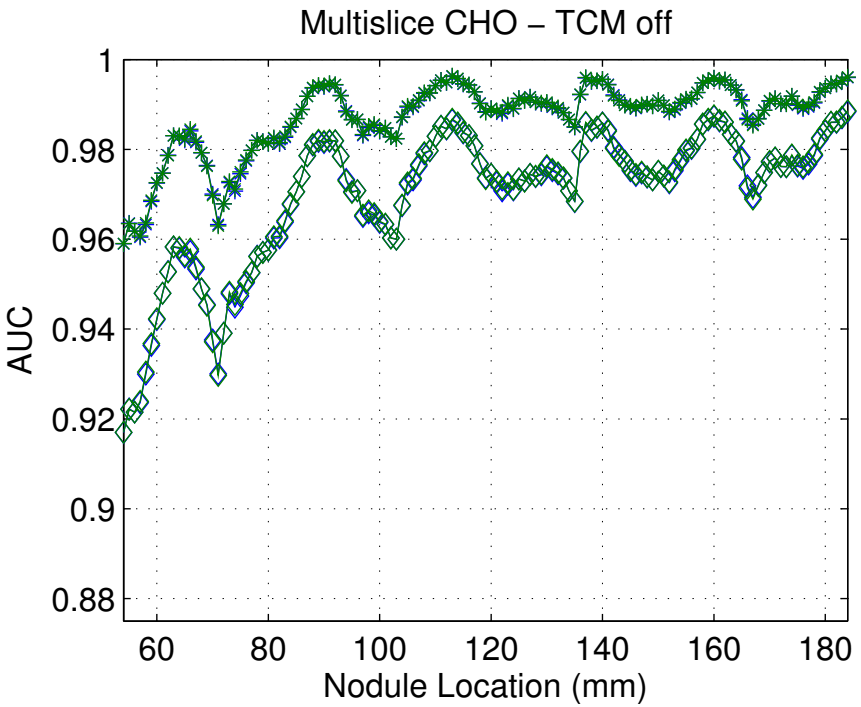

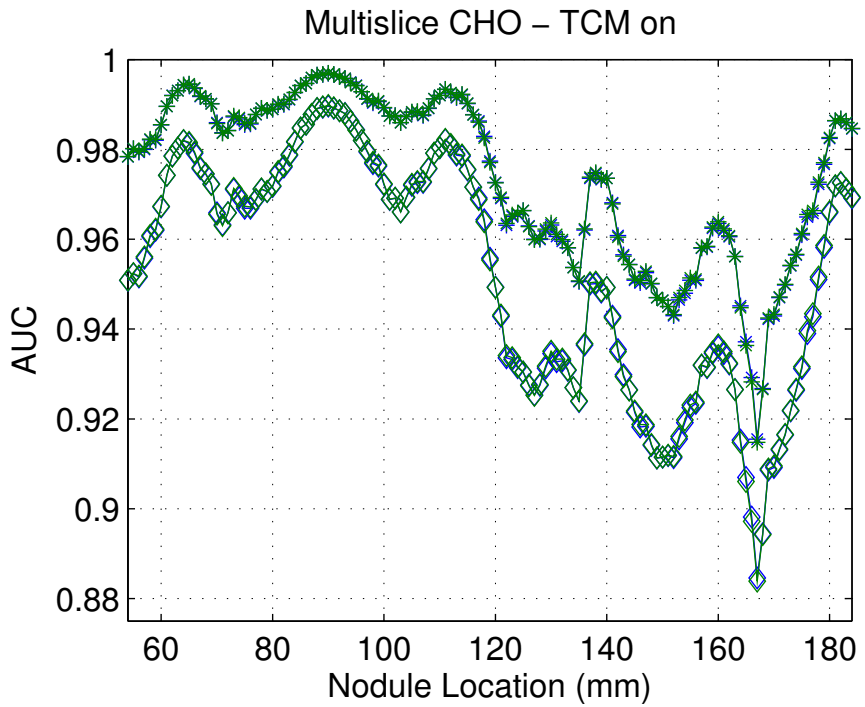

- Detection substantially higher than single-slice observers
- Trends for fixed TC and modulated TC are same as single-slice observers

Summary

- In fixed TC scans, detection is lowest through shoulders, leveling off in lower lung
- In modulated TC scans
  - Highest through shoulders
  - Lowest through lower lung
  - Increasing into the abdomen as TC prospectively increases
  - **Detectability roughly follows TCM profile**

Summary

- In fixed TC scans, detection is lowest through shoulders, leveling off in lower lung
- In modulated TC scans
  - Highest through shoulders
  - Lowest through lower lung
  - Increasing into the abdomen as TC prospectively increases
  - Detectability roughly follows TCM profile

Summary

- In fixed TC scans, detection is lowest through shoulders, leveling off in lower lung
- In modulated TC scans
  - Highest through shoulders
  - Lowest through lower lung
  - Increasing into the abdomen as TC prospectively increases
  - **Detectability roughly follows TCM profile**

TCM overlay

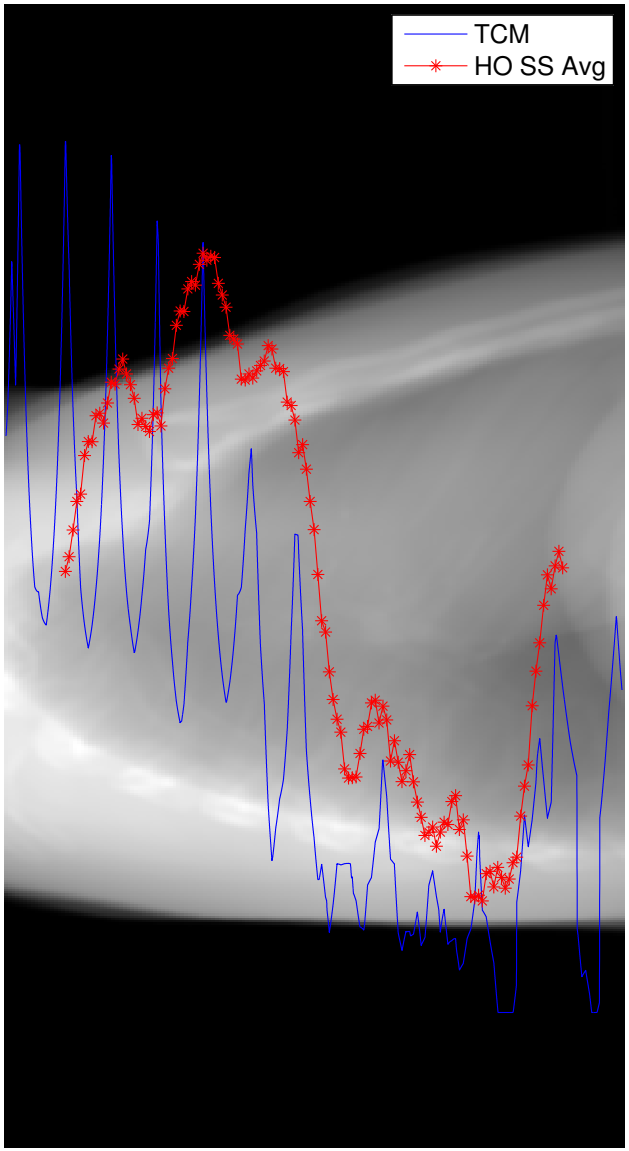

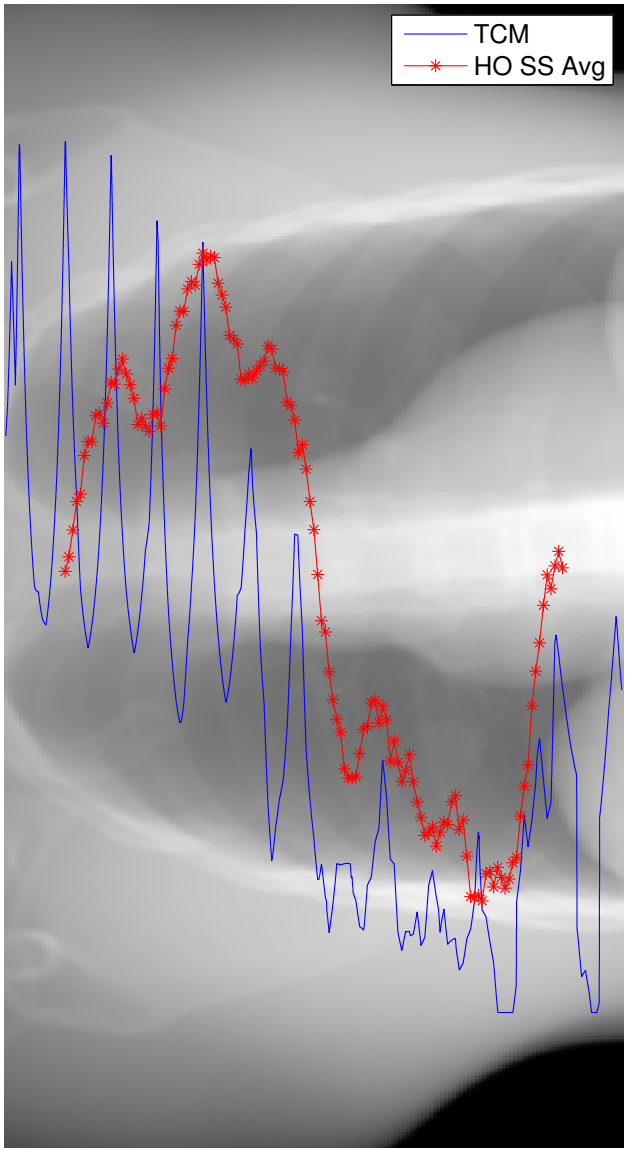

Fixed TC Overlay

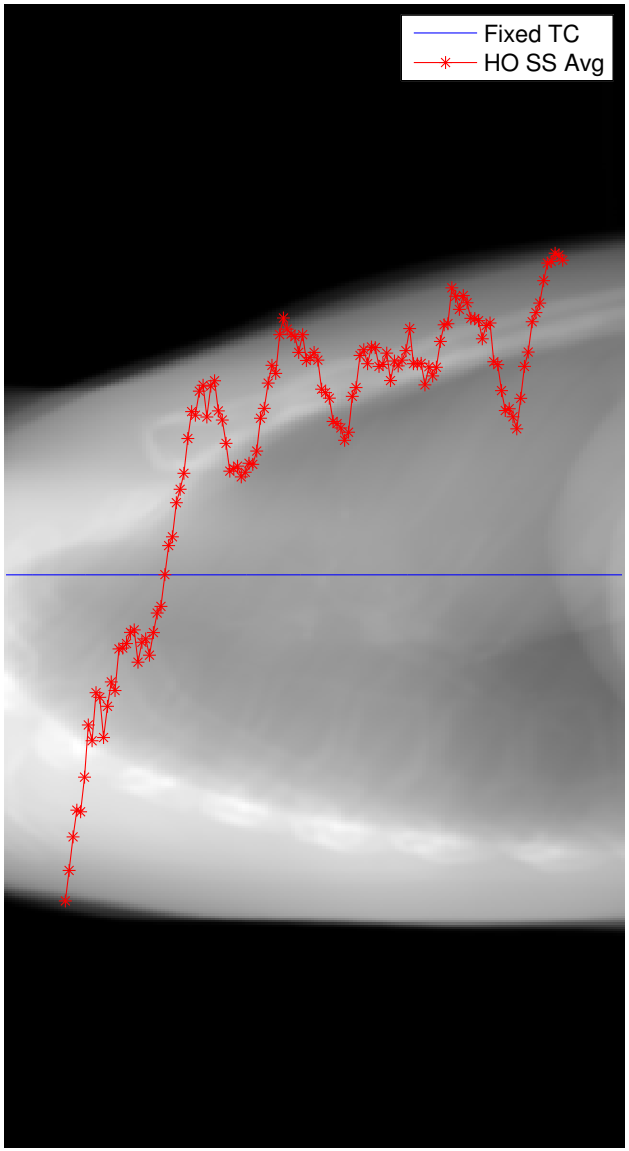

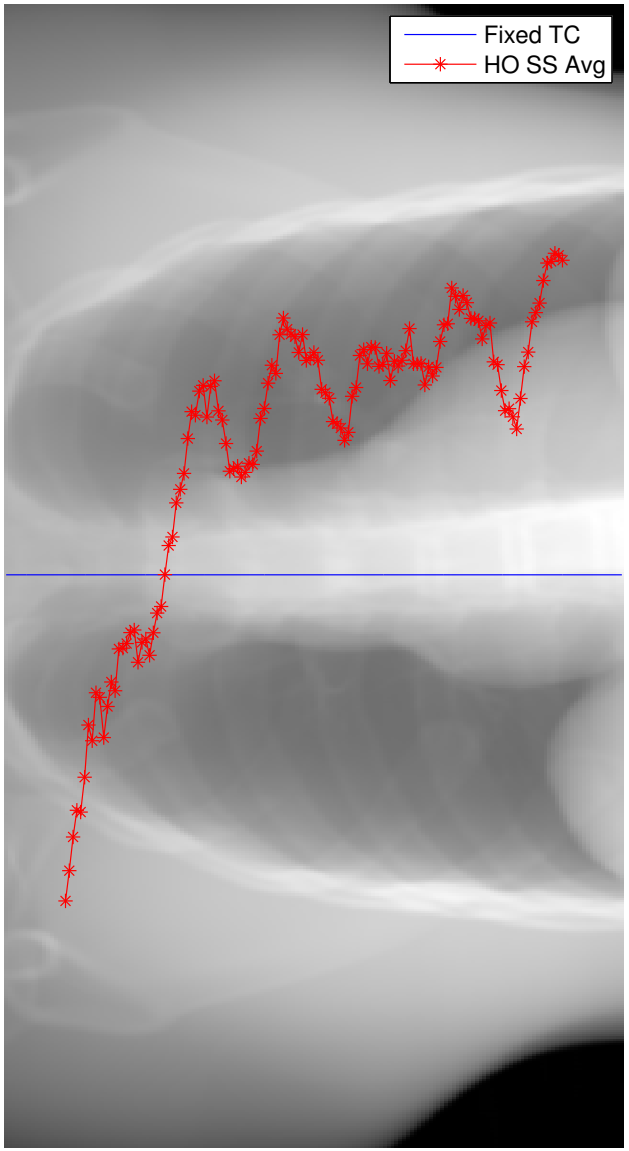

Outline

Discussion

- In this work, TCM **has a non-trivial impact on detection** of difficult, low-contrast lesions
- Consistent detectability behavior between all observers
  - **MO selection did not appear to have a major impact on detectability** trends for this type of task
- While humans may have a hard time detecting 6mm, 25 HU lesions, TCM scheme design will likely impact CAD and quantitative imaging

Discussion

- In this work, TCM **has a non-trivial impact on detection** of difficult, low-contrast lesions
- Consistent detectability behavior between all observers
  - **MO selection did not appear to have a major impact on detectability** trends for this type of task
- While humans may have a hard time detecting 6mm, 25 HU lesions, TCM scheme design will likely impact CAD and quantitative imaging

Discussion

- In this work, TCM **has a non-trivial impact on detection** of difficult, low-contrast lesions
- Consistent detectability behavior between all observers
  - **MO selection did not appear to have a major impact on detectability** trends for this type of task
- While humans may have a hard time detecting 6mm, 25 HU lesions, TCM scheme design will likely impact CAD and quantitative imaging

Limitations

- Task is too "easy" (... for MOs)
  - MOs consistently display very high detectability leading to...
- Task is too difficult (... for humans)
  - 6mm, 25 HU nodule is exceedingly difficult to detect
  - Clinical "relevance" (i.e. to human readers) is perhaps "broken"
- Photon counts are low in lateral projections (3-4 photons in some detectors)
  - Electronic noise
- No anatomical noise

Limitations

- Task is too "easy" (... for MOs)
  - MOs consistently display very high detectability leading to...
- Task is too difficult (... for humans)
  - 6mm, 25 HU nodule is exceedingly difficult to detect
  - Clinical "relevance" (i.e. to human readers) is perhaps "broken"
- Photon counts are low in lateral projections (3-4 photons in some detectors)
  - Electronic noise
- No anatomical noise

Limitations

- Task is too "easy" (... for MOs)
  - MOs consistently display very high detectability leading to...
- Task is too difficult (... for humans)
  - 6mm, 25 HU nodule is exceedingly difficult to detect
  - Clinical "relevance" (i.e. to human readers) is perhaps "broken"
- Photon counts are low in lateral projections (3-4 photons in some detectors)
  - Electronic noise
- No anatomical noise

Limitations

- Task is too "easy" (... for MOs)
  - MOs consistently display very high detectability leading to...
- Task is too difficult (... for humans)
  - 6mm, 25 HU nodule is exceedingly difficult to detect
  - Clinical "relevance" (i.e. to human readers) is perhaps "broken"
- Photon counts are low in lateral projections (3-4 photons in some detectors)
  - Electronic noise
- No anatomical noise

Future work

- More challenging task for the MOs
  - Object classification (vessel/nodule)
  - Search tasks
  - Include anatomical noise
- More clinically realistic task (higher contrast nodules, nodules of varying sizes, etc.)
- Novel TCM optimization schemes for
  - Known nodule location
  - Unknown nodule location
  - Maximize overall detection across whole lung

Future work

- More challenging task for the MOs
  - Object classification (vessel/nodule)
  - Search tasks
  - Include anatomical noise
- More clinically realistic task (higher contrast nodules, nodules of varying sizes, etc.)
- Novel TCM optimization schemes for
  - Known nodule location
  - Unknown nodule location
  - Maximize overall detection across whole lung

Future work

- More challenging task for the MOs
  - Object classification (vessel/nodule)
  - Search tasks
  - Include anatomical noise
- More clinically realistic task (higher contrast nodules, nodules of varying sizes, etc.)
- Novel TCM optimization schemes for
  - Known nodule location
  - Unknown nodule location
  - Maximize overall detection across whole lung

Finally...

Thank you for your interest and any questions!

References I

Chang, B., Hwang, J. H., Choi, Y. H., Chung, M. P., Kim, H., Kwon, O. J., Lee, H. Y., Lee, K. S., Shim, Y. M., Han, J., and Um, S. W. (2013). Natural history of pure ground-glass opacity lung nodules detected by low-dose CT scan. *Chest*, 143(1):172–178.

Gang, G. J., Stayman, J. W., Ehtiati, T., and Siewerdsen, J. H. Task-driven image acquisition and reconstruction in cone-beam CT. *Physics in Medicine & Biology*, 3129:3129.

Hoffman, J., Young, S., Noo, F., and McNitt-Gray, M. (2016). Technical Note : FreeCT _ wFBP : A robust , efficient , open-source implementation of weighted filtered backprojection for helical , fan-beam CT. *Medical physics*, 43(3):10 pp.

Lim, H. J., Ahn, S., Lee, K. S., Han, J., Shim, Y. M., Woo, S., Kim, J. H., Yie, M., Lee, H. Y., and Yi, C. A. (2013). Persistent pure ground-glass opacity lung nodules $\geq$ 10 mm in diameter at CT scan: Histopathologic comparisons and prognostic implications. *Chest*, 144(4):1291–1299.

Mcmillan, K., Bostani, M., Mccollough, C. H., and McNitt-Gray, M. (2015). TU-EF-204-01: Accurate Prediction of CT Tube Current Modulation: Estimating Tube Current Modulation Schemes for Voxelized Patient Models Used in Monte Carlo Simulations. *Medical Physics*, 42:3620.

Platiša, L., Goossens, B., Vansteenkiste, E., Park, S., Gallas, B. D., Badano, A., and Philips, W. (2011). Channelized Hotelling observers for the assessment of volumetric imaging data sets. *Journal of the Optical Society of America A*, 28(6):1145–63.

Segars, W. P., Sturgeon, G., Mendonca, S., Grimes, J., and Tsui, B. M. W. (2010). 4D XCAT phantom for multimodality imaging research. *Medical physics*, 37(9):4902–4915.

References II

Wunderlich, A. and Noo, F. (2008). Evaluation of the impact of tube current modulation on lesion detectability using model observers. *Conference proceedings : ... Annual International Conference of the IEEE Engineering in Medicine and Biology Society. IEEE Engineering in Medicine and Biology Society. Conference*, 2008:2705–8.

Wunderlich, A. and Noo, F. (2011). Confidence intervals for performance assessment of linear observers. *Medical Physics*, 38(S1):S57.